RESEARCH ARTICLE

Dynamic Analysis of the Blood-Brain Barrier Disruption in Experimental Stroke Using Time Domain In Vivo Fluorescence Imaging

Abedelnasser Abulrob, Eric Brunette, Jacqueline Slinn, Ewa Baumann, and Danica Stanimirovic

Abstract

The blood-brain barrier (BBB) disruption following cerebral ischemia can be exploited to deliver imaging agents and therapeutics into the brain. The aim of this study was (a) to establish novel in vivo optical imaging methods for longitudinal assessment of the BBB disruption and (b) to assess size selectivity and temporal patterns of the BBB disruption after a transient focal ischemia. The BBB permeability was assessed using in vivo time domain near-infrared optical imaging after contrast enhancement with either free Cy5.5 (1 kDa) or Cy5.5 conjugated with bovine serum albumin (BSA) (67 kDa) in mice subjected to either 60- or 20-minute transient middle cerebral artery occlusion (MCAO) and various times of reperfusion (up to 14 days). In vivo imaging observations were corroborated by ex vivo brain imaging and microscopic analyses of fluorescent tracer extravasation. The in vivo optical contrast enhancement with Cy5.5 was spatially larger than that observed with BSA-Cy5.5. Longitudinal studies after a transient 20-minute MCAO suggested a bilateral BBB disruption, more pronounced in the ipsilateral hemisphere, peaking at day 7 and resolving at day 14 after ischemia. The area differential between the BBB disruption for small and large molecules could potentially be useful as a surrogate imaging marker for assessing perinfarct tissues to which neuroprotective therapies of appropriate sizes could be delivered.

INTRAVENOUS THROMBOLYSIS is the only approved treatment for acute ischemic stroke, with clear therapeutic benefit when administered within the first 3 hours of stroke onset. The pipeline of neuroprotective therapies aiming to salvage damaged tissue or prolong its survival beyond a 3-hour limit for thrombolysis failed to demonstrate clear clinical benefit. The problem of poor clinical translation is aggravated by the lack of experimental evidence that these therapies truly access their brain targets through the intact or damaged blood-brain barrier (BBB).

Advances in imaging techniques are expected to accelerate the development of therapies for acute ischemic stroke by enabling more accurate initial assessment of the penumbra, better selection and monitoring of patients undergoing thrombolysis, and better patient stratification for clinical trials.[1] Whereas computed tomography (CT) and magnetic resonance imaging (MRI) are routinely used clinically, molecular imaging techniques (eg, single-photon emission computed tomography [SPECT], positron emission tomography [PET], and molecular MRI) currently have a limited role in the evaluation of acute stroke patient owing to a lack of both reliable molecular surrogates of neurologic outcomes and molecular imaging agents. A recent application describes imaging of neuroinflammation in subacute phase of stroke using ultrasmall superparamagnetic iron oxide (USPIO) nanoparticles as macrophage cell-specific MRI contrast agents.[2] The role for optical imaging techniques in evaluating brain perfusion/oxygenation is currently limited to near-infrared spectroscopy, which noninvasively estimates cerebral oxygenation by measuring the absorption of infrared light by tissue chromophores (hemoglobin and cytochrome αa3).[3] The application of optical imaging techniques in vivo has been hindered by poor tissue penetration and high light scattering. These limitations could partly be alleviated by use

From the Cerebrovascular Research Group, Institute for Biological Sciences, National Research Council of Canada, Ottawa, ON.

This work was supported by the National Research Council of Canada and in part by a Heart and Stroke Foundation of Canada grant-in-aid (#T-5824) to D.S.

Address reprint requests to: Abedelnasser Abulrob, PhD, Cerebrovascular Research Group, Institute for Biological Sciences, National Research Council of Canada, 1200 Montreal Road, Ottawa, ON K1A 0R6; e-mail: Abedelnasser.Abulrob@nrc.gc.ca.

DOI 10.2310/7290.2008.00025

of near-infrared light, which allows deeper tissue penetration of several centimeters,[4] and by analyzing the time domain characteristics of the fluorescence rather than its intensity.[5,6] The fluorescence lifetime (τ) of a probe is the time that a probe spends in the excited state before returning to the ground state; τ is an intrinsic parameter of the probe, insensitive to the probe concentration but responsive to the local tissue microenvironment.[7,8]

The endothelium of brain capillaries regulates the exchange of molecules between blood and brain parenchyma. The BBB is of great clinical importance because many brain pathologies, including stroke, are associated with an increase in permeability for molecules of different sizes, leading to vasogenic edema; furthermore, the BBB restricts the access of systemically administered drugs to the brain physically by tight junctions and by active removal by ABC transporters.[9] Therefore, noninvasive studies of regional distribution, size selectivity, and temporal dynamics of the BBB disruption in brain pathologies could help determine whether the intended systemic therapeutic treatments could access parenchymal targets during the development or progression of the disease. The aim of the current study was to develop and validate applications for time domain in vivo optical imaging, with or without optical contrast enhancement, in detecting or localizing stroke-induced brain injury and determining the dynamics and extent of the BBB disruption in experimental stroke model(s).

Materials and Methods

Middle Cerebral Artery Occlusion in Mouse

All procedures using animals were approved by the institutional animal care committee and complied with the guidelines established by the Canadian Council on Animal Care. Male CD-1 mice (23–25 g) were obtained from Charles River and bred locally. Anesthesia was induced with 1.5% isoflurane and maintained with 1.0% isoflurane in 69% N_2O and 30% O_2 using a vaporizer. Mice were subjected to occlusion of the left middle cerebral artery (MCAO) using an intraluminal filament as previously described.[10] Briefly, an 11 mm silicone-coated nylon thread was introduced into the left common carotid artery of an anesthetized mouse and directed into the internal carotid artery until it obstructed blood flow to the middle cerebral artery (MCA). After either a 20- or 60-minute ischemia, animals were briefly reanesthetized, the filament was withdrawn, and wounds were sutured.

Transcranial blood flow measurements were obtained using an Advance Laser Flowmeter (model ALF21, ADVANCE Co., Ltd. Tokyo, Japan). Briefly, under isofluorane anesthesia, the skin covering the skull was retracted. Pinpoint measurements using a 0.5 mm fiberoptic probe were taken through the intact skull on the right and left hemispheres approximately 7 mm lateral to midline and 2 mm posterior to bregma, an area of brain cortex supplied by the MCA. Baseline CBF (cerebral blood flow) values were defined as 100% flow and taken immediately before the start of the internal carotid artery occlusion surgery. After MCAO was initiated, the readings were obtained at 10, 20, 40, 50, and 59 minutes post–thread introduction. Additional readings were taken after the thread was removed at approximately 65, 80, 100, and 120 minutes after the baseline measurement. The mice were kept under anesthesia for the duration of the experiment, and body (rectal) temperature was maintained between 37.0°C and 38°C for 2.5 hours using a homeothermic blanket. Physiologic parameters, including blood pressure, blood gases, and pH, were measured as previously described.[11] Sham-operated mice, which were subjected to the same brain surgery but no MCAO, were used as controls. The consequences of a transient MCAO on the BBB permeability and brain injury were analyzed at different reperfusion times, up to 14 days.

Histochemical Staining with TTC

To visualize the ischemic damage after a transient MCAO, the brains were removed and, using mouse stainless steel coronal brain matrices (Harvard Apparatus Canada, St Laurent, QC), sectioned in four 2 mm thick coronal slices, using the rostral margin of the pons as a landmark. Sections were immersed in a 2% solution of 2,3,5-triphenyltetrazolium chloride (TTC) at 37°C for 15 minutes to promote even staining and then removed from the solution and digitally photographed.[10] The infarct areas lacking TTC staining were measured using image software *Axiovision* 4.6, Zeiss, Toronto, ON) and multiplied with 2 mm thickness for each of four slices to calculate total infarct volume.

In Vivo Time Domain Optical Imaging

A small-animal time domain eXplore Optix MX2 preclinical imager (Advanced Research Technologies, Montreal, QC) was used for in vivo imaging. eXplore Optix enables calculation or reconstruction of both fluorophore depth and concentration using a measured time-resolved fluorescence signal.[12,13]

To evaluate in vivo time domain near-infrared optical imaging in assessing the BBB permeability and/or brain damage, two imaging paradigms were tested in a model of transient MCAO in mice: (a) optical imaging using contrast enhancement with the near-infrared probes and (b) optical imaging without contrast enhancement measuring changes in endogenous fluorophores.

Prior to undergoing MCAO, mice were imaged in eXplore Optix to obtain a background image. Animals subjected to MCAO or reperfusion were injected with either the near-infrared fluorescent probe, Cy5.5 (100 nmol) (molecular weight [MW] = 1 kDa; fluorescence lifetime, $\tau?_{[Cy5.5]}$ = 1.0 ns; GE Healthcare, Milwaukee, WI), or with the same volume of physiologic saline via the tail vein 15 minutes prior to undergoing imaging procedures in eXplore Optix. To determine the BBB disruption for molecules of different sizes, in some studies, bovine serum albumin labeled with Cy5.5 (BSA-Cy5.5, 50 μg intravenous) (MW = 67 kDa) was used for contrast enhancement. Sham-operated animals were also imaged prior to and 15 minutes after the injection of 100 nmol Cy5.5 or at appropriate times after the injection of 50 μg BSA-Cy5.5. In longitudinal studies, where images were obtained repeatedly over a period of time, Cy5.5 (100 nmol) injection was always given 15 minutes prior to imaging (time of the highest signal to background ratio). In all imaging experiments, a 670 nm pulsed laser diode with a repetition frequency of 80 MHz and a time resolution of 12 ps light pulse was used for excitation. The fluorescence emission at 700 nm was collected by a highly sensitive time-correlated single-photon counting system and detected through a fast photomultiplier tube. Each animal was positioned prone on a plate that was then placed on a heated base (36°C) in the imaging system. The optimal elevation of the animal was verified via a side-viewing digital camera. A two-dimensional scanning region encompassing the head was selected via a top-reviewing real-time digital camera. Laser excitation beam controlled by galvomirrors was then moved over the selected region of interest (ROI). Laser power and counting time per pixel were optimized at 60 μW and 0.5 seconds, respectively. The raster scan interval was 1.0 mm and was held constant during the acquisition of each frame; 300 such points were scanned for each ROI. The data were recorded as temporal point-spread functions, and the images were reconstructed as fluorescence intensity (FI), fluorescence lifetime (τ), and fluorescence concentration maps (Conc).

Data Analysis

The background consisting of baseline image acquired in each animal before the induction of ischemic injury was subtracted from each subsequent image. The pre- and postinjection images were automatically coregistered by eXplore Optix *Optiview* 2.1 software (ART Inc, Montreal, QC) to allow for background subtraction. The imaging parameters (FI, τ, and Conc) were measured in each image using the same ROIs in the ischemic left hemisphere and the contralateral right hemisphere. The territory of the infarcted area after MCAO was created using digital maps described in the literature.[14,15] The measured area was adjusted to approximately the same size for each animal.

Normalized FI was represented in arbitrary units (AUs) that reflect photon counts normalized with laser power and integration time and was calculated as photon counts ÷ [laser intensity (μW) × integration time (S)]. Three-dimensional reconstruction software from Advanced Research Technologies was used for the topographic representations of the depth and calculation of Cy5.5 concentration within the animal profile.[16,17] To determine the fluorescence concentration and depth of the fluorophore, time-resolved information was acquired using mouse brain tissue absorption coefficient (mua) and reduced scattering coefficient (musp) values of 0.03 mm^{-1} and 1.5 mm^{-1}, respectively.[18] The analysis focuses on the temporal position of the fluorescence temporal point-spread function maximum, *t*TPSFmax. Under point assumption, *t*TPSFmax at reflection geometry is independent of fluorophore concentration but shifts to later times as the depth of fluorophore increases. Therefore, fluorophore depth can be estimated from *t*TPSFmax value. By comparing the measured fluorescence signal amplitude with the modeled value, the fluorophore concentration is retrieved.[17,18]

To estimate the fluorescence decay, *OptiView* 2.1 software was used.[19] The software deconvolutes the measured fluorescent intensity–time decay curve using

the Levenberg-Marquardt algorithm, which applies a nonlinear least-squares minimization algorithm to compute the coefficients of a multiexponential expansion of the fluorescence decay as described.[12]

Histologic Assessment of Brain Injury

In some experiments, imaging results were confirmed by histochemical analyses in brain sections. After imaging, animals were perfused with heparinized saline and 10% formalin and sectioned using vibrotome into 25 μm thick sections. Neighboring sections were histochemically stained with hematoxylin and eosin (H&E) to identify damaged regions or with the tomato lectin–fluorescein isothiocyanate (FITC) (1:100; 30 minutes) to identify brain vessels and 4',6-diamidino-2-phenylindole (DAPI) (1 μg/mL; 1 minute) to stain cell nuclei. H&E-stained sections were viewed and recorded in phase-contrast mode using an LCM PixCell IIe Microscope. The BBB disruption was assessed by visualizing Cy5.5 extravasation into brain parenchyma using a Zeiss Axiovert 200 fluorescent microscope (Carl Zeiss, Maple Grove, MN) in a near-infrared mode (a 660 to 680 nm excitation filter and a 700 nm longpass emission filter). Image processing was performed using *AxioVision LE Rel* 4.4 software.

Statistical Analysis

Data are shown as the means ± SD of fluorescence intensity or fluorescence concentration. Statistical analyses of differences between ischemic and contralateral ROIs were performed using one-way analysis of variance (ANOVA) followed by a Tukey post hoc test or a Student two-tailed *t*-test, as indicated; *p* values less than .05 were considered significant.

Results

Cy5.5 Contrast-Enhanced In Vivo Imaging of the Transient MCAO

The near-infrared dye Cy5.5 does not cross the intact BBB in vitro (data not shown) or in vivo (the experimental demonstration of this can be seen in Figure 6B). The dye is rapidly cleared from the circulation, mainly through kidney excretion. Given that transient MCAO has been shown to produce BBB disruption for both small molecules such as gadolinium and large molecules such as albumin,[20] Cy5.5 and BSA-Cy5.5 were used as small and large MW optical tracers, respectively, to localize ischemic stroke based on the tracer tissue extravasation. A similar principle is applied in MRI diffusion imaging of stroke using contrast enhancement with gadolinium.[21] In the first series of experiments, a 60-minute MCAO followed by a 24-hour reperfusion was used because it produces a reproducible infarction affecting a large part of the lateral striatum and parietal cortex,[22] as well as moderate BBB disruption for macromolecules.[23] The experimental protocol is shown schematically in Figure 1A. A uniform reduction of rCBF (Regional cerebral blood flow) over the ischemic region to below 20% of preischemic values was measured in all animals subjected to MCAO at the end of a 60-minute occlusion; immediately after thread removal, rCBF recovered to ≈70% of preischemic values and remained at these levels over 1 hour of reperfusion (data not shown). The measured rCBF values demonstrated minimal variability across experimental groups (data not shown) and were similar to those reported in the literature in the same ischemia model.[23] Cy5.5 was injected intravenously 15 minutes prior to imaging, and two imaging parameters, FI and Conc, were then acquired and analyzed in the hemispheric ROIs (Figure 1, B–D). The FI signal showed clear lateralization to the left (ischemic) side of the brain (see Figure 1B); the measured average FI of the ischemic hemisphere in six separate animals was 3,580 ± 50 AU compared with 730 ± 35 AU in the contralateral hemisphere ($p < .01$; *t*-test; each ROI = 150 points); FI values in the right hemisphere were similar to preischemic baseline levels (700 ± 25 AU) and to values measured in Cy5.5-injected sham-operated animals (740 ± 30 AU). This observation confirmed that the majority of Cy5.5 was cleared from the circulation 15 minutes after injection.

Unlike other optical imaging techniques, time domain optical imaging enables coupling of the relative fluoroprobe concentration with the tissue depth, allowing a three-dimensional reconstruction and virtual optical tomography. Topographic three-dimensional representation of the axial (*x*-axis), sagittal (*y*-axis), and coronal (*z*-axis) volume planes of the head (see Figure 1C) and optical coronal sectioning in 1 mm thickness increments (see Figure 1D) showed the highest Cy5.5 concentration at a depth of 6 to 9 mm (measured from the top of the head profile) in the ischemic hemisphere (Figure 1D). In an 8 to 9 mm optical section (enlarged image in Figure 1D), Cy5.5 concentration measured in scanned points indicated

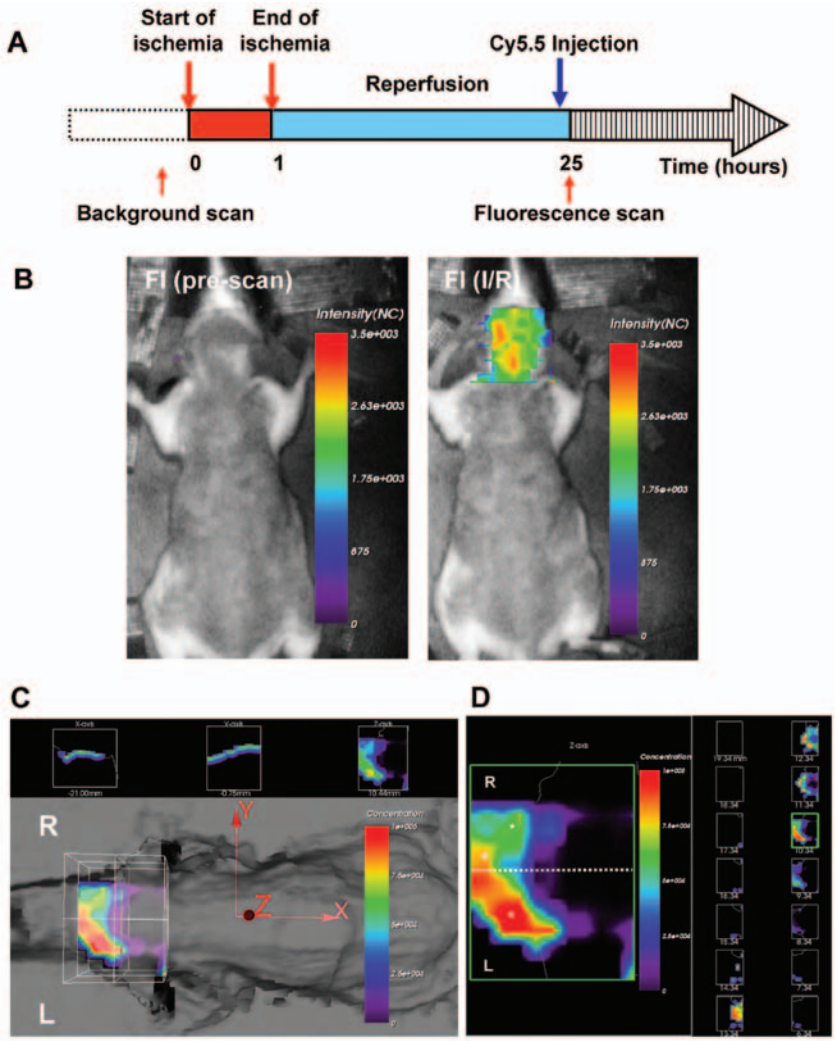

Figure 1. Representative in vivo images of the head region of interest (ROI) in animals subjected to a transient 60-minute middle cerebral artery occlusion followed by a 24-hour reperfusion and injected with Cy5.5 (100 nmol; 15 minutes prior to imaging). Images were acquired using an eXplore Optix time domain pre clinical imager. *A*, Schematic of the experimental imaging protocol used in these experiments. *B*, Representative images of fluorescence intensity (FI) in the head ROI prior to and after ischemia/reperfusion (I/R). *C*, The reconstruction of the head concentration volumetric planes (showing three sections through the head: coronal [*x*], sagittal [*y*], and axial [*z*]) superimposed on the three-dimensional image of the animal head profile. *D*, *Z*-axis sectioning (20 1 mm sections) through the thickness of the head. The highest signal (enlarged image) was detected in an 8 to 9 mm depth section from the top of the head profile. The results are representative of experiments performed in six animals.

by stars was 10-fold higher in the ischemic compared with the contralateral side. Elevated Cy5.5 concentration signal was also measured in the right hemisphere adjacent to the brain midline (in the area marked with a cross on Figure 1D).

Histologic Confirmation of Cy5.5 Extravasation

The extent of infarction caused by the 60-minute MCAO followed by 24-hour reperfusion was evaluated in TTC-stained thick brain slices (Figure 2A). The histochemical confirmation of neuronal damage was done by H&E staining, using criteria developed by Farber and colleagues,[24] whereas Cy5.5 extravasation was assessed by fluorescence microscopy, in brain sections roughly corresponding to brain regions depicted in thick brain slices. As shown in Figure 2B, sections from the ischemic hemisphere, corresponding to thick slices 1, 2, and 3 (see Figure 2A), showed typical signs of neuronal necrosis, whereas sections corresponding to thick slice 4 (see Figure 2A) appeared similar to the

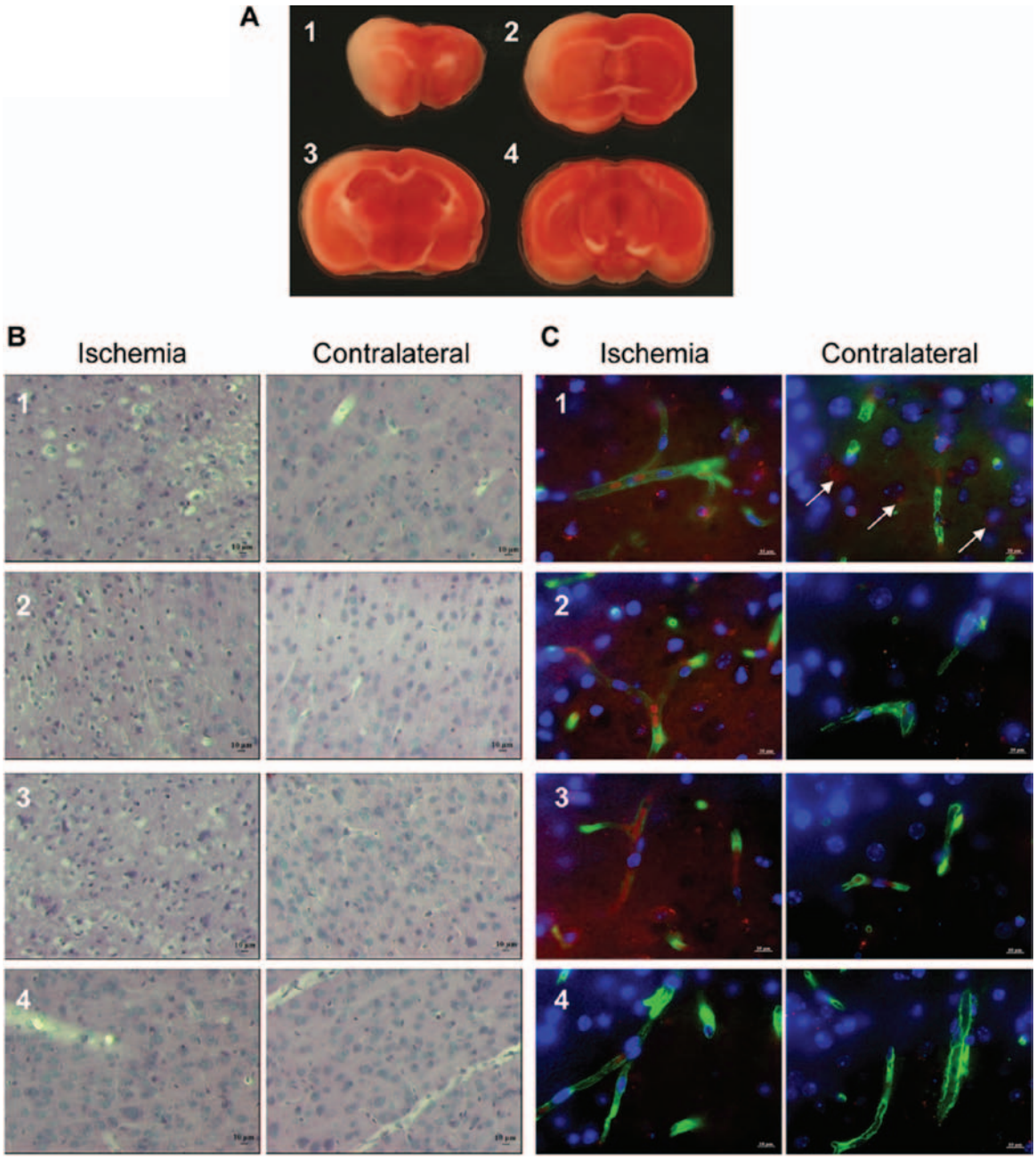

Figure 2. *A*, Representative images of TTC-stained brain slices 24 hours after a 60-minute middle cerebral artery occlusion. Histologic (*B*) and fluorescent microscopy (*C*) analyses of the ischemic and contralateral sides in 25 μm sections of brain slices (1–4) were performed as described in Materials and Methods. Brain vessels were visualized using FITC–tomato lectin (*green*), and cellular nuclei were stained with DAPI (*blue*). Extravasation of Cy5.5 signal (*red*) in the contralateral side is shown by *arrows*. Scale bar = 10 μm. The results are representative of experiments performed in six animals.

contralateral hemisphere. In adjacent sections counterstained with vessel-binding lectin (green) (Figure 2C), the Cy5.5 (red signal) extravasation into the brain parenchyma was extensive on the ischemic side in sections corresponding to thick slices 1 to 3 but not in sections corresponding to thick slice 4 (see Figure 2, A and C). Interestingly, some Cy5.5 parenchymal extravasation was consistently observed in the contralateral hemisphere in sections corresponding to thick slice 1 (see Figure 2C1, white arrows), even in

the absence of the histologic evidence of neuronal damage. A residual intravascular Cy5.5 fluorescence, observed predominantly on the ischemic side, is likely owing to poorer perfusion of ischemic vessels.

BSA-Cy5.5 Contrast-Enhanced In Vivo Imaging of the Transient MCAO

To determine size selectivity of the BBB permeability after a 60-minute MCAO, 50 μg of BSA-Cy5.5 was injected intravenously immediately after MCAO, and animals were imaged at 1, 3, and 24 hours of reperfusion (Figure 3A). Because the circulation half-life of BSA-Cy5.5 is much longer than that of Cy5.5, only one injection was needed for a longitudinal study of up to 24 hours. Figure 3 shows FI signal in the head ROI in sham-operated (upper panels) and ischemic (lower panels) animals at indicated times after BSA-Cy5.5 injection. In animals subjected to MCAO (Figure 3, B and C), the average FI signal increased 2.5-fold in the left compared with the right hemisphere

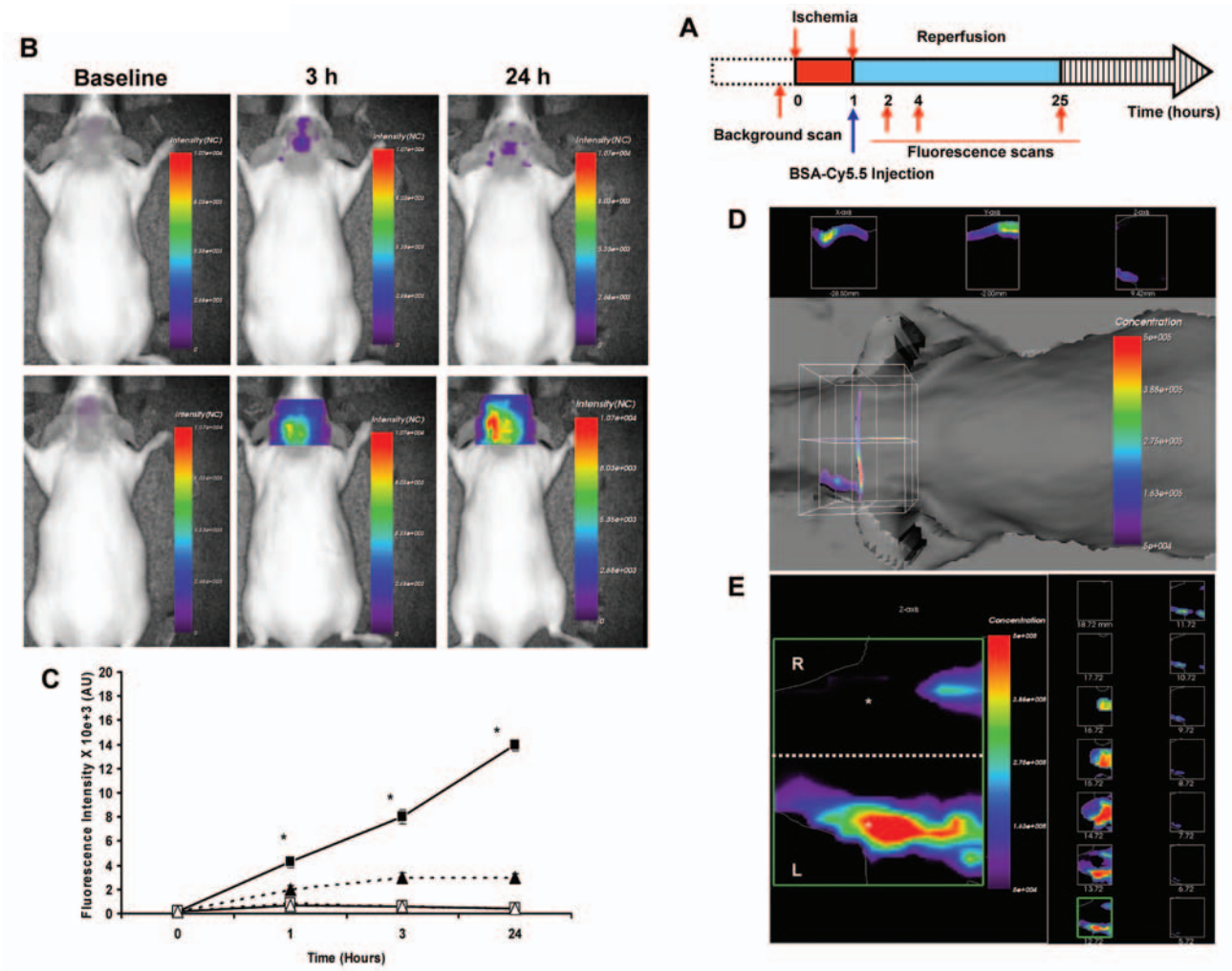

Figure 3. Representative in vivo images of the head region of interest (acquired using eXplore Optix) in animals subjected to a transient 60-minute middle cerebral artery occlusion (MCAO) followed by 24-hour reperfusion and injected with 50 μg BSA-Cy5.5. *A*, Schematic of the experimental imaging protocol used in these experiments. *B*, Representative images of fluorescence intensity (FI) in sham-operated mice (*upper panels*) and mice that had undergone MCAO (*bottom panels*) at indicated time points of reperfusion. *C*, Quantitative analysis of FI in the left ischemic (*black squares*) and right contralateral (*black triangles*) brain hemisphere after MCAO and left (*open squares*) and right (*open triangles*) hemispheres of sham-operated animals at indicated times of reperfusion. Each point is mean ± SD of FI values obtained from six animals. *Asterisks* indicate significant differences ($p < .05$; ANOVA) between the left and right hemispheres. *D*, The reconstruction of the in vivo head concentration volumetric planes (showing coronal [*x*], sagittal [*y*], and axial [*z*] planes) superimposed on the three-dimensional image of the animal head profile. *E*, *Z*-axis sectioning (20 1 mm sections) through the thickness of the head. The enlarged image is 6 to 7 mm depth section from the top of the head profile.

at 3 hours and was markedly (4.5-fold) elevated at 24 hours of reperfusion. The signal in the nonischemic hemisphere was slightly but not significantly elevated compared with sham-operated animals at 24 hours of reperfusion (Figure 3D). Owing to the long plasma half-life of BSA-Cy5.5, contrast enhancements observed in the ischemic hemisphere over 24 hours reflect brain accumulation kinetics of the contrast rather than the BBB permeability status at different time points.

Topographic three-dimensional representation of the axial (*x*-axis), sagittal (*y*-axis), and coronal (*z*-axis) volume planes (sections) of the head (see Figure 3D) and optical tomography in 1 mm thickness increments (Figure 3E) both show a distinct lateralization of the BSA-Cy5.5 signal to the left hemisphere 24 hours after MCAO. In optical sections corresponding to 6 to 7 mm depth from the top of the head profile (enlarged image in Figure 3E), the BSA-Cy5.5 concentration signal was completely lateralized to the left hemisphere corresponding to the MCA territory and was not detectable in the right hemisphere (see Figure 3E, depicted by stars). The signal observed in the posterior part of the head profile bilaterally originated from glands and soft tissues in submandibular and neck regions, where large MW BSA-Cy5.5 is present for prolonged periods of time.

Volumetric Analyses in Brains Imaged Ex Vivo

In brains imaged ex vivo, volumetric comparisons of the fluorescence concentration signals for Cy5.5 and BSA-Cy5.5 were performed using three-dimensional reconstruction and optical sectioning. Optical sectioning for Cy5.5 concentration signal through the *x*-, *y*-, and *z*-axes is shown in Figure 4A. A fourfold increase in the Cy5.5 concentration signal was measured in the ischemic core region compared with the periphery of the infarct (shown by a star and a cross, respectively, in the *z*-section in Figure 4A), and a 12.5-fold difference was observed between the ischemic core and the contralateral hemisphere (shown by a star and an x, respectively, in the z-section of Figure 4A). BSA-Cy5.5 concentration enhancement localized exclusively to the left hemisphere in planar sections and in three-dimensional reconstruction (Figure 4, B and C). The volumes of contrast enhancement, calculated by multiplying the enhancement area in each slice with the thickness of the slice, were (71 ± 11 mm^3) and (44 ± 7 mm^3) for Cy5.5 and BSA-Cy5.5, respectively ($p < .01$, *t*-test). The infarct volume measured from TTC staining in separate animals subjected to a 60-minute MCAO, and 24-hour reperfusion was 43.61 ± 0.98 mm^3, similar to values reported in the literature.[25]

In contrast to Cy5.5 extravasation observed in tissue sections in the contralateral hemisphere (see Figure 3), no BSA-Cy5.5 extravasation was detected in contralateral hemisphere by fluorescent microscopy analyses (data not shown). Although the majority of the fluorescent enhancement signal measured in brains ex vivo likely originated from the extravasated (parenchymal) tracer, we cannot exclude that the residual intravascular tracer contributed to contrast enhancement in these analyses.

In Vivo Imaging of Transient MCAO without Contrast Enhancement

Given that fluorescence lifetimes of endogenous fluorophores can change in response to alterations in tissue microenvironment, we next examined whether brain injury produced by a transient MCAO (60 minutes followed by 24-hour reperfusion) can be detected by in vivo time domain fluorescence imaging without contrast enhancement. Whereas the endogenous FI was similar in the left and right hemispheres prior to MCAO (Figure 5A and Table 1), the left ischemic hemisphere showed significantly ($p < .05$) higher average endogenous FI than the contralateral hemisphere after MCAO (see Figure 5A and Table 1).

Similarly, the average weighted fluorescence lifetime, τ_{av}, for the ischemic hemisphere increased significantly when compared with preischemic values (see Figure 5A and Table 1). The normalized intensity–time decay curves for left and right hemispheres prior to and after MCAO are shown in Figure 5b1 and Figure 5b2, respectively; τ decay was slower in the ischemic hemisphere. Endogenous FI and τ_{av} in the brain ex vivo were significantly elevated in ischemic hemisphere (see Table 1). Therefore, both endogenous FI and τ_{av} identified ischemic regions as single parameters in vivo and ex vivo.

Longitudinal Assessment of BBB Permeability after Mild MCAO

To evaluate the usefulness of time domain optical imaging in assessing longitudinal changes in the BBB permeability after MCAO, we used a transient 20-minute MCAO insult shown to produce small

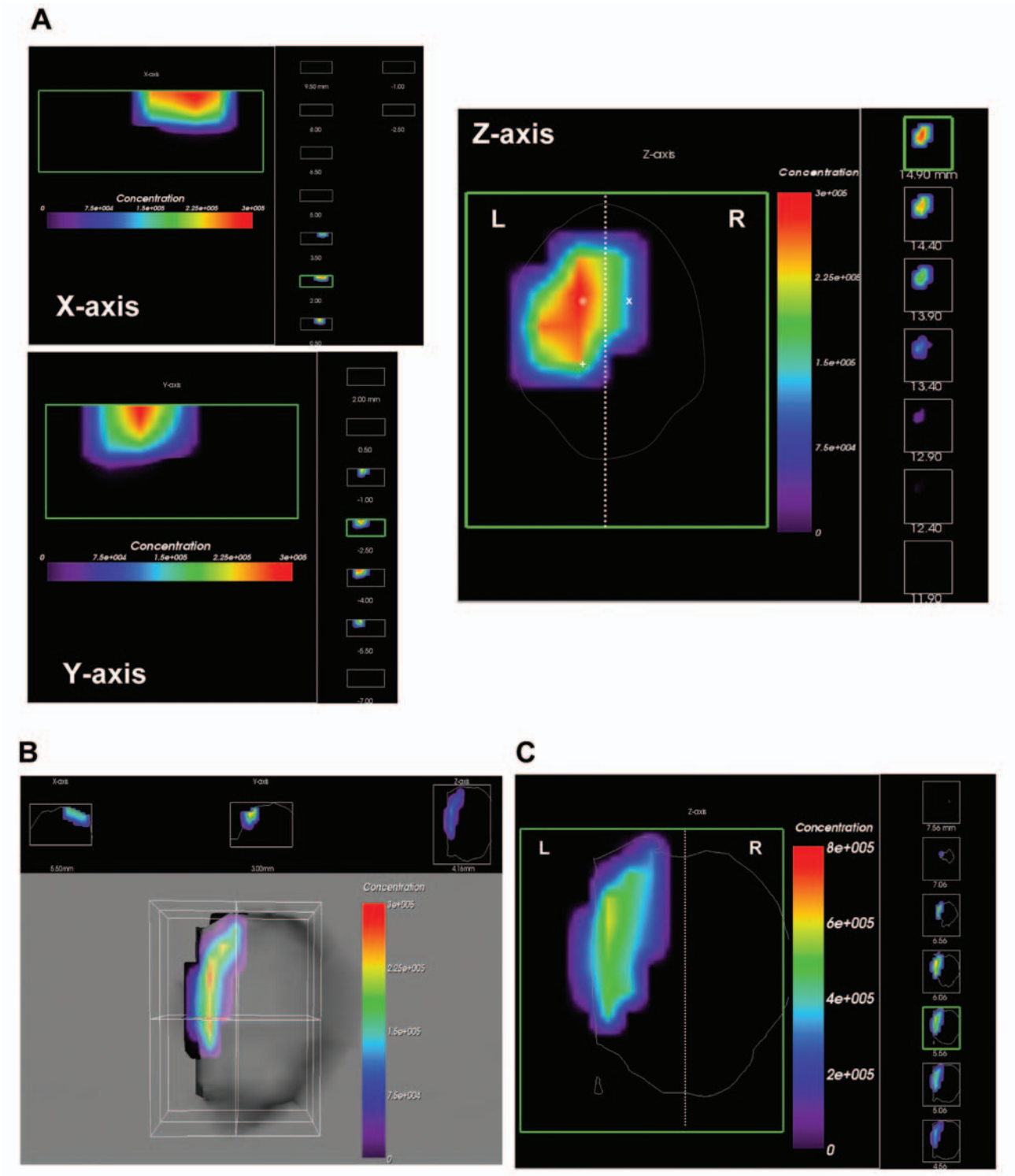

Figure 4. Representative ex vivo brain images (obtained in eXplore Optix) of animals subjected to a transient 60-minute middle cerebral artery occlusion followed by a 24-hour reperfusion and injected with either Cy5.5 (100 nmol, 15 minutes prior to imaging) (*A*) or BSA-Cy5.5 (50 μg, 24 hours prior to imaging) (*B* and *C*). *A*, Axial (*z*), coronal (*x*), and sagittal (*y*) axis sectioning through the thickness of the ex vivo brain (optical tomography) showing Cy5.5 signal distribution in volumetric planes. *B*, Representative ex vivo reconstructions of the volumetric planes (coronal [*x*], sagittal [*y*], and axial [*z*]) of BSA-Cy5.5 distribution. *C*, Z-axis sectioning through the thickness of the ex vivo brain showing complete lateralization of Cy5.5-BSA signal to the left (L) hemisphere. The results are representative of experiments performed in six animals.

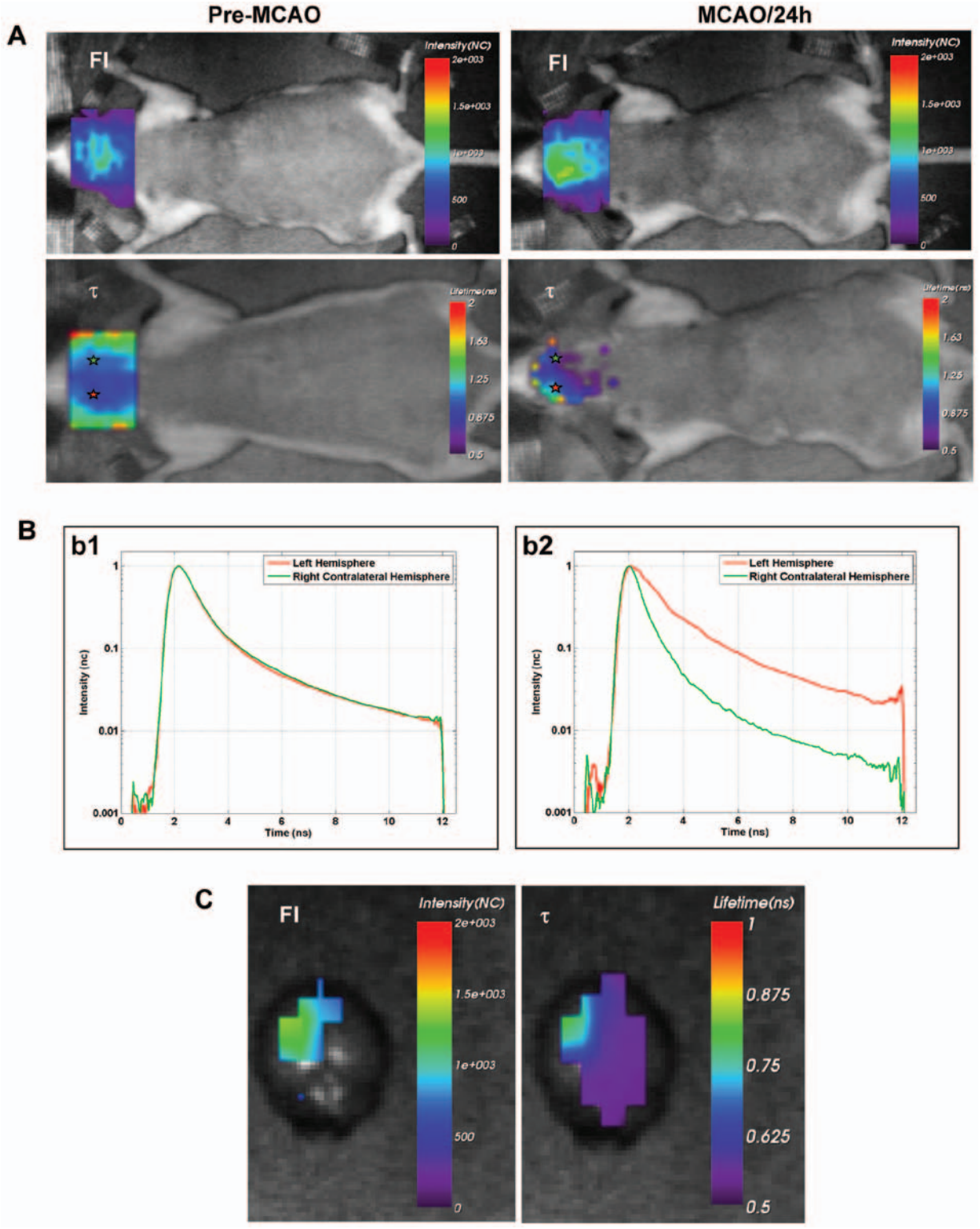

Figure 5. *A*, Representative images of the endogenous fluorescence intensity (FI) and fluorescence lifetime (τ) in head regions of interest before and 24 hours after a 60-minute middle cerebral artery occlusion (MCAO). *B*, The normalized intensity–time decay curves comparing left (*red*) and right (*green*) brain hemispheres prior to MCAO (b1) and 24 hours after MCAO (b2). Pixels selected for analysis are shown in *red and green stars* superimposed on images in *A*. *C*, Representative endogenous FI and τ images of ex vivo brains from *A*. The results are representative of experiments performed in six animals.

Table 1. Endogenous Fluorescence Intensity (FI) and Lifetime (τ) Values Measured in the Left and Right Hemisphere ROI In Vivo Before and After a Transient Left MCAO Followed by 24 h of Reperfusion. Animals Were Injected with 50 μL of Saline at the End of Reperfusion and were Imaged in eXplore Optix 15 min after Saline Injection.

	Left		*Right*	
	FI [AU]	τ_{av} *[ns]*	*FI [AU]*	τ_{av} *[ns]*
In vivo				
Before MCAO	800 ± 20	1.0 ± 0.1	850 ± 30	1.0 ± 0.1
After MCAO	1180 ± 25*†	1.3 ± 0.1*	930 ± 35	0.9 ± 0.1
Ex vivo				
Sham	800 ± 25	0.5 ± 0.1	800 ± 25	0.5 ± 0.1
After MCAO	1000 ± 20*	0.9 ± 0.1*	800 ± 15	0.5 ± 0.1

Fluorescence lifetime analysis was performed using double exponential Levenberg-Marquard algorithm. Fluorescence intensity, FI is given in arbitrary units. τ_{av} - average weighed fluorescence lifetime. Values are means ± SD after background subtraction, $n = 6$ per group.
* - indicates $p < 0.05$ (t-test) between left and right brain hemispheres. † - indicates $p < 0.05$ (t-test) between values prior to and after MCAO.

damage affecting subcortical structures and white matter,[26] which enabled longer animal survival for longitudinal studies up to 14 days.

Because extravasated Cy5.5 cleared from brain over 24 hours (data not shown), leaving no residual signal, it was possible to estimate the BBB permeability status longitudinally using repeated injections of Cy5.5, provided that the injection intervals were longer than 24 hours (Figure 6A). In sham-operated animals, vascular endothelium was impermeable to Cy5.5 (Figure 6B). Concentration/depth coupling in three-dimensional reconstruction (see Figure 6B) showed dynamic, bilateral changes in Cy5.5 concentrations over 14 days of reperfusion. Lateralization of the Cy5.5 concentration signal was observed in the left hemisphere (see Figure 6B) at 24 hours; further signal increases in both left and right hemispheres were observed 7 days after MCAO; 14 days after MCAO, the signal was essentially the same as in the sham-operated animals bilaterally (see Figure 6B). Quantitative analyses of the Cy5.5 concentration signal after a mild transient MCAO are shown in Figure 6C; the signal detected in the ischemic hemisphere was always significantly higher than that in the contralateral hemisphere (see Figure 6C).

Discussion

This study describes the first application of the time domain optical imaging in a noninvasive in vivo evaluation of the localization, progression, and resolution of the experimental stroke. This technique, unlike continuous wave– and frequency domain–based optical imaging techniques, enables coupling of the optical tracer concentration with the tissue depth, as well as measurements of fluorescence lifetime of exogenous or endogenous fluorophores. Although it lacks in spatial resolution, the sensitivity of the technique in experimental setting surpasses that of the small-animal MRI by several magnitudes, enabling detection of subtle changes in tracer concentrations.[27] The advent of in vivo multiphoton microscopy, which uses excitation at near-infrared wavelengths and allows in vivo imaging at submicron resolution and at depths of several hundred microns below the brain surface, recently enabled elegant studies of the cerebrovascular system.[28] However, despite high resolution, in vivo multiphoton microscopy remains essentially an invasive technique that requires opening of the cranial window and is therefore suitable for analyses of spatially limited brain regions and not applicable in prospective studies of the disease. This study demonstrates that time domain optical imaging technique could reliably detect brain infarct lesions in experimental models and, owing to its high sensitivity, could provide information on the extent and dynamics of the BBB disruption after stroke in a noninvasive and prospective manner.

The brain capillary endothelium under physiologic conditions allows selective entry of key nutrients but prevents a majority of circulating compounds, includ-

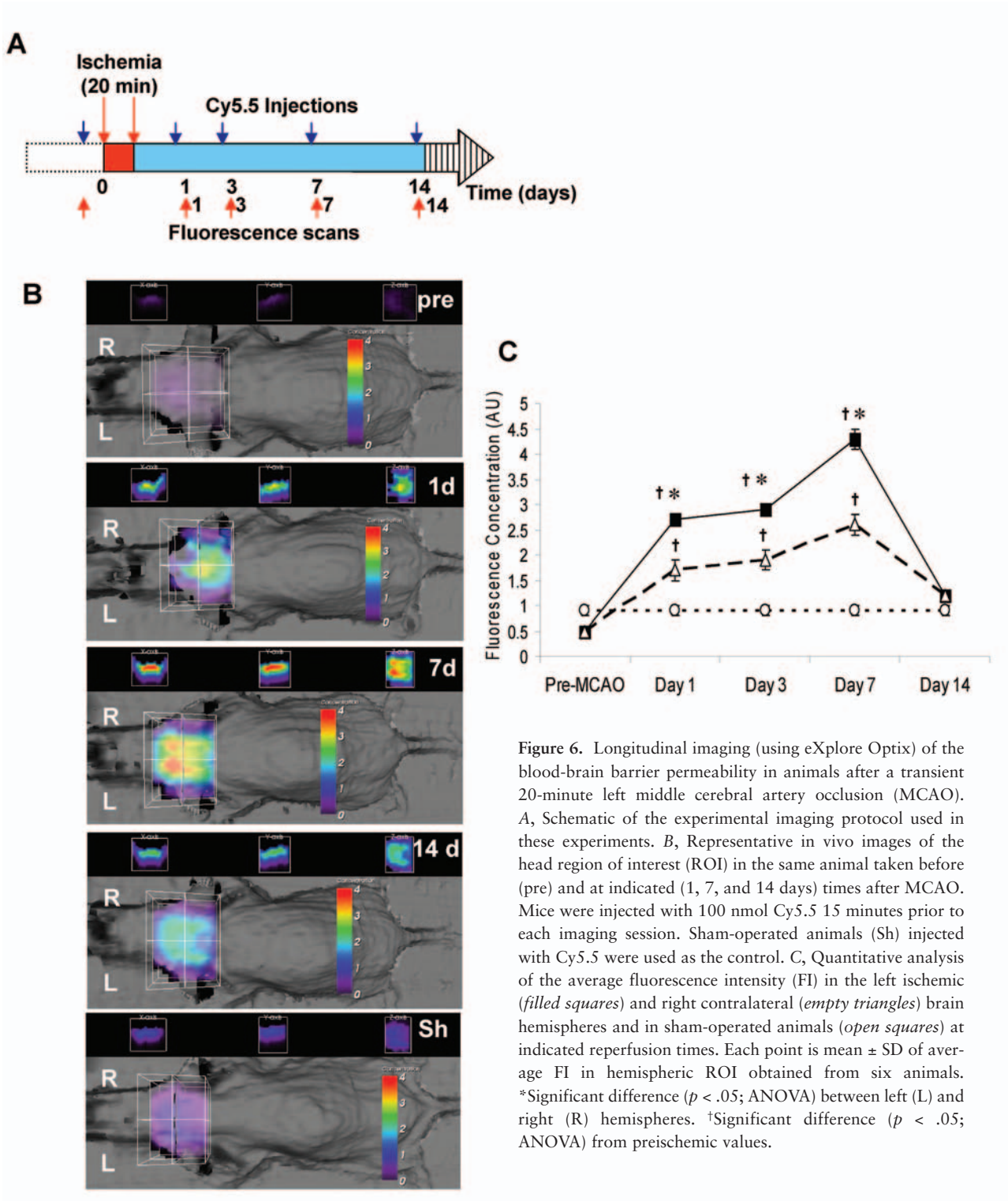

Figure 6. Longitudinal imaging (using eXplore Optix) of the blood-brain barrier permeability in animals after a transient 20-minute left middle cerebral artery occlusion (MCAO). *A*, Schematic of the experimental imaging protocol used in these experiments. *B*, Representative in vivo images of the head region of interest (ROI) in the same animal taken before (pre) and at indicated (1, 7, and 14 days) times after MCAO. Mice were injected with 100 nmol Cy5.5 15 minutes prior to each imaging session. Sham-operated animals (Sh) injected with Cy5.5 were used as the control. *C*, Quantitative analysis of the average fluorescence intensity (FI) in the left ischemic (*filled squares*) and right contralateral (*empty triangles*) brain hemispheres and in sham-operated animals (*open squares*) at indicated reperfusion times. Each point is mean ± SD of average FI in hemispheric ROI obtained from six animals. *Significant difference ($p < .05$; ANOVA) between left (L) and right (R) hemispheres. †Significant difference ($p < .05$; ANOVA) from preischemic values.

ing therapeutic drugs and contrast agents, from reaching the brain.[29] The BBB disruption caused by stroke, inflammatory brain diseases, traumatic brain injury, or brain tumors has been exploited to deliver imaging agents such as gadolinium into the brain and produce contrast enhancement depicting brain lesions and surrounding brain edema. However, surprisingly little is known about the temporal dynamics, spatial distribution, and size selectivity of the BBB disruption during the course of ischemic brain injury. The recent consen-

sus article on strategies to advance translational research in this field identified "quantification of the time-course of barrier breakdown to molecules of different sizes after different types of neurotrauma as a research priority."[30] This article describes a novel experimental in vivo molecular imaging technique applicable in prospective monitoring of the BBB permeability and ischemic injury; using this technique, we determined size selectivity of the BBB disruption after a severe MCAO, as well as temporal dynamics of the BBB disruption after a mild MCAO.

In the first application of the time domain optical imaging described in the study, it was clearly demonstrated that 24 hours after a 60-minute MCAO, the BBB is disrupted for both small and large MW tracers in ischemic brain regions; this can be reliably imaged in vivo as fluorescence intensity enhancement and increased optical probe concentration on the side of cerebral infarct. In vivo observations were corroborated by demonstrated extravasation of Cy5.5 in brain sections using fluorescence microscopy.

Comparisons of Cy5.5 and BSA-Cy5.5 revealed no molecular size restriction of the BBB for two tracers in the ischemic core 24 hours after MCAO. However, analyses from three-dimensional reconstruction indicated that, in contrast to BSA-Cy5.5, the free Cy5.5 concentration signal was also enhanced in the contralateral hemisphere, especially in frontal regions adjacent to the brain midline. This observation suggested that, after MCAO, the BBB permeability for the large MW tracer was roughly limited to areas demarcated as infarcted by TTC staining, whereas the small MW tracer had wider spatial distribution compared with both the large MW tracer and TTC-demarcated infarct volume. In brains imaged ex vivo after perfusion, differences between Cy5.5- and BSA-Cy5.5-enhanced territories were slightly less extensive than those observed in vivo, suggesting that optical signal in vivo could contain some artifacts from light scattering from the skull and skin. Microscopically, Cy5.5 extravasation was also consistently confirmed in the contralateral anterior frontal sections.

Variations in the spatial distribution and size selectivity of the BBB disruption in stroke have been suggested by earlier studies. Studies in rats using radiolabeled tracers showed that transfer constants for sucrose (342 Da) were three times higher than those of larger inulin (5,000 Da) 6 hours after a transient global cerebral ischemia[31] or 24 hours after a transient 2-hour focal ischemia.[32] A recent study demonstrated spatially more distributed areas of MRI enhancement for gadolinium–diethylenetriaminetetraacetic acid (Gd-DTPA) (550 Da) compared with Gd-DTPA linked to BSA and Evans blue (68 kDa) 24 hours after a 3-hour MCAO in rats.[20] Concurrent changes in $T_{1\text{-sat}}$ were larger in the Gd-BSA-EB (Evan's blue)-enhancing areas than in the Gd-DTPA-enhancing areas, suggesting that greater BBB damage was a major factor contributing to the observed differences in contrast enhancement.

Although analogous interpretation of data presented in this study is attractive and could infer possible use of the spatial differential between the BBB permeability for small and large MW tracers as a surrogate imaging biomarker of penumbra, similar to the diffusion perfusion mismatch model in MRI analysis,[33] some shortcomings of these studies preclude definitive conclusions. Although in this study, in contrast to that of Nagaraja and colleagues,[20] two imaging tracers, Cy5.5 and BSA-Cy5.5, were assessed in separate groups of animals, unequal delivery of two contrast agents owing to local perfusion differences was unlikely given minimal interanimal variability in measured rCBF. However, as discussed by Nagaraja and colleagues,[20] diffusion of large BSA-Cy5.5 in the brain extracellular space could be more restricted than that of Cy5.5 owing to cytotoxic brain edema and astrocytic swelling.

Dynamic temporal changes in the BBB permeability have been described in experimental models of cerebral ischemia. For example, transient global cerebral ischemia is characterized by a biphasic BBB opening, peaking at 1 and 24 hours and receding at 6 hours after reperfusion.[34] Each BBB disruption event is accompanied with distinct changes in expressed cerebrovascular proteins: loss of ion transporters and energy-driven pumps at 1 hour and increased expression of inflammatory and angiogenic proteins at 24 hours.[34] Temporal patterns of the BBB disruption after a transient mild MCAO measured using longitudinal optical imaging studies showed a surprising resemblance to the biphasic pattern observed in global ischemia models, albeit over prolonged timelines; the ipsilateral Cy.5.5 contrast enhancement measured by fluorescence concentration at different depths was significantly elevated at 24 hours, plateaued at 3 days, and was secondarily increased 7 days after MCAO. Interestingly, this study also identified significant

increases in the BBB permeability for Cy5.5 in the contralateral hemisphere; the BBB disruption for Cy5.5 in both ipsi- and contralateral hemispheres resolved by 14 days after mild MCAO. Literature studies on the BBB permeability changes after mild experimental MCAO over prolonged periods of time are lacking; however, lasting BBB pathology (over years) is common in patients after mild traumatic brain injury[35] and correlates with neuronal activity. A comprehensive analysis of a 20-minute MCAO in the mouse by Miyashita and colleagues[26] demonstrated "maturation" (ie, augmentation) in both infarct size and gliosis on the ipsilateral side over at least 7 days after the insult, as well as an increased number of PECAM-1-positive cells, indicating increased capillary density, between days 7 and 56 after the insult. These changes could conceivably underlie prolonged BBB disruption for Cy5.5 after the same insult observed in this study using in vivo imaging.

Imaging techniques that provide information on the metabolic status of the "tissue at risk" surrounding stroke (penumbra) prior to and after therapeutic intervention, as currently attempted by a combination of perfusion and diffusion MRI, would be beneficial in acute stroke management. The endogenous fluorescence lifetime-τ is a potentially novel imaging parameter that can provide additional information on the tissue status in vivo because it is sensitive to tissue microenvironment, including tissue pH, hypoxia, or ischemia. Interestingly, both endogenous FI and τ were significantly altered in ischemic brain regions compared with either sham-operated animals or the contralateral hemisphere, allowing for reliable detection of the ischemic stroke even in the absence of contrast injection. The reasons for these changes remain speculative; although they may be caused by brain edema owing to the BBB disruption (measured by contrast-enhanced methods), they also could reflect metabolic perturbations in the ischemic or damaged tissue. In our recent study of renal ischemia/reperfusion,[12] multiexponential decay analyses of endogenous τ reliably identified ischemic kidney in vivo. Better understanding of microenvironment perturbations that cause changes in endogenous FI and τ is necessary for further validation of τ as a molecular imaging indicator of metabolically stressed tissues. Time-resolved diffuse optical tomographic imaging has recently been shown to provide both anatomic and functional information about biologic tissues in human diagnostic setting.[36] Noninvasive imaging of endogenous optical tissue parameters, including τ, is currently used clinically for breast cancer diagnosis.[37]

Experimental applications of the time domain in vivo imaging in stroke described in this study could facilitate the development of new imaging techniques and surrogate markers for monitoring occurrence, progression, and recovery from stroke. The extent of cerebrovascular damage during and after an ischemic event is a positive indicator of cerebral edema, hemorrhagic transformation, and worsened outcomes in stroke patients.[38] The noninvasive evaluation of size-selective BBB permeability changes during the progression and resolution of ischemic stroke could be a useful surrogate indicator of stroke severity and therapeutic delivery or efficacy.

Acknowledgment

We would like to thank Mr. Tom Devesceri for his help with graphic and image processing.

References

1. Kidwell CS, Hsia AW. Imaging of the brain and cerebral vasculature in patients with suspected stroke: advantages and disadvantages of CT and MRI. Curr Neurol Neurosci Rep 2006;6:9–16.
2. Saleh A, Schroeter M, Ringelstein A, et al. Iron oxide particle-enhanced MRI suggests variability of brain inflammation at early stages after ischemic stroke. Stroke 2007;38:2733–7.
3. Tobias JD. Cerebral oxygenation monitoring: near-infrared spectroscopy. Expert Rev Med Devices 2006;3:235–43.
4. Ntziachristos V, Ripoll J, Wang LV, Weissleder R. Looking and listening to light: the evolution of whole-body photonic imaging. Nat Biotechnol 2005;23:313–20.
5. Bloch S, Lesage F, Mclntosh L, et al. Whole-body fluorescence lifetime imaging of a tumor-targeted near-infrared molecular probe in mice. J Biomed Opt 2005;10:054003.
6. Day RN, Schaufele F. Imaging molecular interactions in living cells. Mol Endocrinol 2005;19:1675–86.
7. Lakowicz JR, editor. Principle of fluorescence spectroscopy. 2nd ed. New York: Kluwer Academic/Plenum Publishers; 1999.
8. Elson D, Requejo-Isidro J, Munro I, et al. Time-domain fluorescence lifetime imaging applied to biological tissue. Photochem Photobiol Sci 2004;3:795–801.

9. Pardridge WM. Drug and gene delivery to the brain: the vascular route. Neuron 2002;36:555–8.
10. MacManus JP, Fliss H, Preston E, et al. Cerebral ischemia produces laddered DNA fragments distinct from cardiac ischemia and archetypal apoptosis. J Cereb Blood Flow Metab 1999;19:502–10.
11. MacManus JP, Jian M, Preston E, et al. Absence of the transcription factor E2F1 attenuates brain injury and improves behavior after focal ischemia in mice. J Cereb Blood Flow Metab 2003;23:1020–8.
12. Abulrob A, Brunette E, Slinn J, et al. In vivo time domain optical imaging of renal ischemia-reperfusion injury: discrimination based on fluorescence lifetime. Mol Imaging 2007;6:304–14.
13. Ma G, Delorme J, Gallant P, Boas D. Comparison of simplified Monte Carlo simulation and diffusion approximation for fluorescence signal from phantoms with typical mouse tissue optical properties. Appl Opt 2007;46,1686–92.
14. Phan TG, Donnan GA, Wright PM, Reutens DC. A digital map of middle cerebral artery infarcts associated with middle cerebral artery trunk and branch occlusion. Stroke 2005;36:986–91.
15. Damasio HA. Computed tomographic guide to the identification of cerebral vascular territories. Arch Neurol 1983;40:138–42.
16. Bloch S, Xu B, Ye Y, et al. Targeting beta-3 integrin using a linear hexapeptide labeled with a near-infrared fluorescent molecular probe. Mol Pharm 2006;3:539–49.
17. Hall D, Ma G, Lesage F, Wang Y. Simple time-domain optical method for estimating the depth and concentration of a fluorescent inclusion in a turbid medium. Opt Lett 2004;29:2258–60.
18. Ma G, Gallant P, Mclntosh L. Sensitivity characterization of a time-domain fluorescence imager: eXplore Optix. Appl Opt 2007;46:1650–7.
19. Lam S, Lesage F, Intes X. Time-domain fluorescent diffuse optical tomography: analytical expressions. Optics Express 2005;13:2263–75.
20. Nagaraja TN, Karki K, Ewing JR, et al. Identification of variations in blood-brain barrier opening after cerebral ischemia by dual contrast-enhanced magnetic resonance imaging and T1sat measurements. Stroke 2008;39:427–32.
21. Latour LL, Kang DW, Ezzeddine MA, et al. Early blood-brain barrier disruption in human focal brain ischemia. Ann Neurol 2004;56:468–77.
22. Belayev L, Busto R, Zhao W, et al. Middle cerebral artery occlusion in the mouse by intraluminal suture coated with poly-L-lysine: neurological and histological validation. Brain Res 1999;833:181–90.
23. Mao Y, Yang G-Y, Zhou L-F, et al. Focal cerebral ischemia in the mouse: description of a model and effects of permanent and temporary occlusion. Mol Brain Res 1999;63:366–70.
24. Farber JL, Chien KR, Mittnacht S. Myocardial ischemia: the pathogenesis of irreversible cell injury in ischemia. Am J Pathol 1981;102:271–81.
25. Türeyen K, Vemuganti R, Sailor KA, Dempsey RJ. Infarct volume quantification in mouse focal cerebral ischemia: a comparison of triphenyltetrazolium chloride and cresyl violet staining techniques. J Neurosci Methods 2004;139:203–7.
26. Miyashita K, Itoh H, Arai H, et al. The neuroprotective and vasculo-neuro-regenerative roles of adrenomedullin in ischemic brain and its therapeutic potential. Endocrinology 2006;147:1642–53.
27. Dharmarajan S, Schuster DP. Molecular imaging of the lungs. Acad Radiol 2005;12:1394–405.
28. Vérant P, Serduc R, van der Sanden B, et al. Subtraction method for intravital two-photon microscopy: intraparenchymal imaging and quantification of extravasation in mouse brain cortex. J Biomed Opt 2008;13:011002.
29. Pardridge WM Blood-brain barrier biology and methodology. J Neurovirol 1999;5:556–9.
30. Neuwelt E, Abbott NJ, Abrey L, et al. Strategies to advance translational research into brain barriers. Lancet Neurol 2008;7:84–96.
31. Preston E, Webster J. Differential passage of [14C] sucrose and [3H] inulin across rat blood-brain barrier after cerebral ischemia. Acta Neuropathol (Berl) 2002;103:237–42.
32. Huang ZG, Xue D, Preston E, et al. Biphasic opening of the blood-brain barrier following transient focal ischemia: effects of hypothermia. Can J Neurol Sci 1999;26:298–304.
33. Kidwell CS, Alger JR, Saver JL. Beyond mismatch: evolving paradigms in imaging the ischemic penumbra with multimodal magnetic resonance imaging. Stroke 2003;34:2729–35.
34. Haqqani AS, Nesic M, Preston E, et al. Characterization of vascular protein expression patterns in cerebral ischemia/reperfusion using laser capture microdissection and ICAT-nanoLC-MS/MS. FASEB J 2005;19:1809–21.
35. Tomkins O, Shelef I, Kaizerman I, et al. Blood-brain barrier disruption in post-traumatic epilepsy. J Neurol Neurosurg Psychiatry 2008;79:774–7.
36. Zhao H, Gao F, Tanikawa Y, et al. Time-resolved diffuse optical tomographic imaging for the provision of both anatomical and functional information about biological tissue. Appl Opt 2005;44:1905–16.
37. Intes X. Time-domain optical mammography SoftScan: initial results. Acad Radiol 2005;12:934–47.
38. Mikulis DJ. Functional cerebrovascular imaging in brain ischemia: permeability, reactivity, and functional MR imaging. Neuroimaging Clin North Am 2005;15:667–80.